Accepted Manuscript

Title: Molecular Mechanisms of the Action of Sphingomyelin-Specific Pore-Forming Toxin, Lysenin

Authors: Neval Yilmaz, Akiko Yamaji-Hasegawa, Françoise Hullin-Matsuda, Toshihide Kobayashi

PII: S1084-9521(16)30450-5
DOI: http://dx.doi.org/doi:10.1016/j.semcdb.2017.07.036
Reference: YSCDB 2299

To appear in: *Seminars in Cell & Developmental Biology*

Received date: 2-6-2017
Revised date: 18-7-2017
Accepted date: 19-7-2017

Please cite this article as: Yilmaz Neval, Yamaji-Hasegawa Akiko, Hullin-Matsuda Françoise, Kobayashi Toshihide.Molecular Mechanisms of the Action of Sphingomyelin-Specific Pore-Forming Toxin, Lysenin.*Seminars in Cell and Developmental Biology* http://dx.doi.org/10.1016/j.semcdb.2017.07.036

Molecular Mechanisms of the Action of Sphingomyelin-Specific Pore-Forming Toxin, Lysenin

Neval Yilmaz[a,b]*, Akiko Yamaji-Hasegawa[a,c], Françoise Hullin-Matsuda[a,d], Toshihide Kobayashi[a,e]*

[a] Lipid Biology Laboratory, RIKEN, Wako, Saitama 351-0198, Japan

[b] Enzyme Research Team, CSRS, RIKEN, Wako, Saitama 351-0198, Japan

[c] Laboratory for Molecular Membrane Neuroscience, BSI, RIKEN, Wako, Saitama 351-0198, Japan

[d] Univ-Lyon, CarMeN laboratory, Inserm U1060, INRA U1397, Université Claude Bernard Lyon 1, INSA Lyon, 69621, Villeurbanne, France

[e] UMR7213 CNRS, Laboratoire de Biophotonique et Pharmacologie, Faculté de Pharmacie, Université de Strasbourg, 74 route du Rhin, 67401 Illkirch, France

Corresponding Authors

* Enzyme Research Team, CSRS, RIKEN, Wako, Saitama 351-0198, Japan
E-mail: nevaly@riken.jp

* UMR7213 CNRS, Laboratoire de Biophotonique et Pharmacologie, Faculté de Pharmacie, Université de Strasbourg, 74 route du Rhin, 67401 Illkirch, France
Phone: +33 3 68 85 42 44
E-mail: toshihide.kobayashi@unistra.fr

ABSTRACT Lysenin, which is an earthworm toxin, strongly binds to sphingomyelin (SM). Lysenin oligomerizes on SM-rich domains and can induce cell death by forming pores in the membrane. In this review, the assembly of lysenin on SM-containing membranes is discussed mostly on the basis of the information gained by atomic force microscopy (AFM). AFM data show that lysenin assembles into a hexagonal close packed (hcp) structure by rapid reorganization of its oligomers on an SM/cholesterol membrane. In case of a phase-separated membrane of SM, lysenin induces phase mixing as a result of pore formation in SM-rich domains, and consequently its hcp assembly covers the entire membrane. Besides the lytic action, lysenin is important as a SM marker and its pore has the potential to be used as a biosensor in the future. These points are also highlighted in this review.

KEYWORDS: lysenin; pore-forming toxin; sphingomyelin; atomic force microscopy; hexagonal close packed; oligomer; prepore; pore; phase coexistence; phase boundary; phase mixing

ABBREVIATIONS: PFT, pore-forming toxin; SM, sphingomyelin; Chol, cholesterol; AFM, atomic force microscopy; TEM, transmission electron microscopy; hcp, hexagonal close packed; DOPC, dioleoylphosphatidylcholine; DPPC, dipalmitoylphosphatidylcholine; DLPC, dilauroylphosphatidylcholine; Lo, liquid ordered; Ld, liquid disordered; EqII, equinatoxin II; CDC, Chol-dependent cytolysin; NT-lysenin, non-toxic lysenin; PIP2, phosphatidylinositol bisphosphate; SMS, SM synthase; GST, glutathione-S-transferase; MBP, maltose-binding protein; nanoSIMS, nanoscale secondary ion mass spectrometry

1. Introduction

Lysenin is a pore-forming toxin (PFT) from the aerolysin family **[1]**. Lysenin was originally purified from the coelomic fluid of earthworm *Eisenia fetida* as a protein that causes contraction of rat vascular smooth muscle **[2]**. Lysenin has also been shown to possess hemolytic and cytolytic activities **[3]**. Molecular cloning of this protein revealed that lysenin is composed of 297 amino acids and two homologous proteins to lysenin are present in *E. fetida* **[4,5]**. While lysenin appears as a 41-kDa band in SDS-PAGE, the molecular mass of lysenin is 33 kDa from gel filtration chromatography and mass spectrum analysis, which is consistent with the molecular weight calculated from the sequence. Lysenin induces the hemolysis of erythrocytes from various animals, which is inhibited by preincubation of the protein with sphingomyelin (SM)-containing liposomes **[3,6]**. Among animal species tested, sheep erythrocytes, which lack phosphatidylcholine and instead are highly enriched with SM, were most sensitive to lysenin. These results suggest the possibility that SM is the target of lysenin. The specific binding of lysenin to SM has been demonstrated through a variety of approaches including ELISA, TLC immunostaining assay, liposome lysis assay and surface plasmon resonance analysis **[3]**. The association of lysenin with SM-containing membranes occurs rapidly and the dissociation is extremely slow, yielding a low dissociation constant (K_d = 5.3 nM). Both the hydrophilic choline headgroup and the hydrophobic hydrocarbon tails of SM are necessary for its interaction with lysenin, indicating the strict lipid specificity in lysenin binding.

Upon binding to SM, lysenin forms oligomers, leading to pore formation on model and cell membranes. The oligomerization of lysenin is certainly facilitated by the presence of cholesterol (Chol) in SM-containing membranes, whereas its binding to SM is only slightly affected by Chol **[3,6,7]**. Fatty acid composition of SM also influences the oligomerization of lysenin, but not the binding of lysenin to SM. At 37 °C, lysenin oligomerizes in the presence of palmitoyl (C16:0) SM, stearoyl (C18:0) SM, palmitoleoyl (C16:1) SM, oleoyl (C18:1) SM or brain SM. In contrast, at 4 °C, only C16:1 SM and C18:1 SM facilitate oligomerization. These results suggest that the membrane fluidity affects the oligomerization step of lysenin **[6]**. The organization of isolated lysenin oligomer was biochemically studied through antibody scanning analysis using anti-peptide antibodies established against synthetic peptides based on the amino acid sequence of lysenin **[6]**. Antibodies raised against the C-terminus of lysenin strongly recognized lysenin oligomer, while antibodies against the N-terminus detected only monomer, suggesting that the C-terminal domain of lysenin is exposed and the N-terminal domain is hidden in the oligomeric complex. The truncated lysenin mutant lacking the N-terminal 160 amino acids still binds to SM specifically, but loses the toxicity **[8]**.

Consequently, the C-terminal domain of lysenin (161~297) is necessary for binding to SM, while the N-terminal domain (1~160) takes part in pore formation.

This review focuses on the assembly of lysenin on both homogenous and phase- separated membranes of SM, visualized using atomic force microscopy (AFM). AFM was used to study the assembly of a wide variety of PFTs on planar lipid membranes. These studies were reviewed recently **[9,10]**. Here, the assembly of lysenin on lipid membranes is discussed in detail on the basis of the findings obtained by AFM observation and other techniques. The significance of lysenin in biology and biotechnology, apart from its toxic action, is also mentioned.

2. Lysenin assembly on a homogeneous membrane of SM

2.1. Structure of lysenin assembly

The structure of the assembly of lysenin oligomers was first revealed by transmission electron microscopy (TEM) **[6]**. The TEM images showed that lysenin oligomers arrange into a honeycomb-like structure on liposomes of SM/Chol (1/1) (mol/mol). With the emergence of the high-speed AFM technique **[11,12]**, the assembly pathway of this honeycomb-like structure could be visualized under physiological conditions at high spatio-temporal resolution **[13]**.

In **Figure 1A**, a high-resolution AFM image of an assembly of lysenin oligomers on a planar membrane of SM/Chol (1/1) (mol/mol) mixture is shown. Each round feature with an inner hole corresponds to an oligomer. The arrangement of lysenin oligomers is a hexagonal close packed (hcp) structure. In this arrangement, oligomers of different heights exist. The tall and short oligomers are assigned as prepores and pores, respectively. The nomination “pore” is used to refer to the membrane-inserted oligomer, however, the possibility of partial insertion is not ruled out because of the presence of a solid support beneath the planar lipid bilayer. The effect of the solid support on PFT assembly was discussed in a recent review article **[9]**. The existence of prepores implies that oligomerization is essential for the membrane insertion of the toxin. This is a common assembly pathway for β-PFTs, which form a β-barrel to span the membrane **[14,15]**. The heights of lysenin oligomers in prepore and pore states were measured to be around 11 and 8 nm, respectively **[16]**. The prepore height is consistent with the length of the water-soluble lysenin monomer **[1]**. This suggests that lysenin protomers in prepore state are oriented in a straight position on the membrane surface, as depicted in **Figure 1B**. The difference between the prepore and pore heights was found to be up to 3 nm. The AFM observation of other β-PFTs, such as perfringolysin O, suilysin and listeriolysin O, also showed a significant reduction in oligomer height upon prepore-to-pore transition **[17-19]**.

The pore structure and the mechanism of pore formation by lysenin were carefully examined in two recent studies conducted by collecting single particle cryo-electron microscopy (cryo-EM) or x-ray diffraction (XRD) data **[20,21]**. The analysis of the crystal structure of the oligomeric pore of wild-type lysenin **[20]** or mutant lysenin, lacking the five negative charges in the transmembrane region (Glu84Gln, Glu85Lys, Glu92Gln, Glu97Ser and Asp126Gly) **[21]**, revealed that each lysenin oligomer consists of nine subunits. The nonameric assembly of lysenin was also confirmed by AFM imaging which was performed under physiological conditions for wild-type lysenin incubated with SM/Chol (1/1) (mol/mol) membrane **(Figure 1C)**. The consistency of results obtained for both wild-type and mutant lysenin using different techniques and under different experimental conditions denotes that "nonamer" is energetically the most favorable oligomeric assembly for lysenin. In the nonameric pore, each protomer is divided into three domains: the C-terminal, N-terminal and β-hairpin domains **(Figure 2A)**. While the C-terminal domains of each protomer are bound to the phosphocholine heads of three SM molecules through electrostatic interactions, nine β-hairpins are formed by unfurling of a significant portion of the N-terminal domains. As shown in **Figure 2B,** the C-terminal and N-terminal domains constitute the cap and collar of the mushroom-shaped pore, whose central stem is built of a long β-barrel. The β-barrel extends from the top to the bottom of the pore, different from hemolysins and aerolysin, although lysenin is a member of the aerolysin family **[22-24]**.

A comparison of the crystal structure of lysenin nonamer with AFM data shows that the diameter of the pore crystal structure, measured to be ~12 nm, agrees well with that obtained from the AFM data **[20,21]**. According to the AFM data, the lateral dimensions of prepores and pores are similar. This might imply that C-terminal domains remain intact during prepore-to-pore transition. By superimposition of the C-terminal domains of the water-soluble monomers and the protomers in the pore state **[21]**, the vertical collapse was found to be ~2 nm, which is consistent with the height reduction observed by AFM. According to the crystal structure, the prepore and pore heights from the membrane surface are ~9 and ~7 nm, respectively. These values are shorter than the prepore and pore heights measured in the course of assembly of lysenin on the phase-separated membrane of SM/dioleoyl- phosphatidylcholine (DOPC)/Chol (2/2/1) (mol/mol/mol) **[16]**. This difference might be resulting from the existence of a viscous water layer surrounding the oligomers or a possible deformation in the membrane. The high concentration of pores in the SM-rich domains might have induced membrane deformation, leading to the increase in the height difference between the SM-rich domains and the oligomer-free DOPC-rich phase, and consequently an increase in the oligomer height relative to the oligomer-free regions of the membrane.

Another point that is worth mentioning about the structure of lysenin assembly is the existence of incomplete arc-shaped oligomers **(Figure 1A)**, as observed for other β-PFTs **[9,10]**. The SM/Chol (1/1) (mol/mol) membrane preincubated with lysenin prior to AFM imaging contained arc-shaped oligomers both in prepore and pore states **[13]**. However, the majority of the arc-shaped oligomers of lysenin was in prepore state. The existence of arcs in pore state implies that the incomplete oligomers can also convert to pores and once they collapse they do not grow further even in the presence of excess monomer. The arc-shaped pores, which have a proteolipidic structure, are also functional, *i.e.*, they can damage the cell membrane **[25,26]**. The analysis of arc-shaped oligomers revealed that they exhibit the same curvature with the complete oligomers and consist of mostly four, five and six subunits **[21]**. The subunit number distribution of arcs denotes that "monomer" is the growth unit in the oligomerization of lysenin, as suggested for the assembly of α-hemolysin and Chol-dependent cytolysins (CDCs) **[27,28]**.

The population of the arc-shaped oligomers of lysenin is very low **[13,21]**, unlike CDCs, which form large oligomers **[10]**. The low oligomerization number or small oligomer size might be one of the factors in the formation of an ordered assembly of lysenin, with a low population of arcs, as observed for α-hemolysin **[29]**. In addition to the small size of lysenin oligomers, which are nonamers, the high fluidity and tight packing of lipids in the liquid-ordered SM/Chol membrane may suppress the concentration of arcs by increasing the oligomerization rate and slowing down the transition from prepores to lower energy-state pores **[30]**. In a recent study, it is suggested that oligomerization should be step-wise and reversible to promote the formation of complete oligomers **[31]**. Thus, the low concentration of arcs may indicate that lysenin oligomerization is both step-wise and reversible at early stages of assembly.

2.2. Mechanism of lysenin assembly into an ordered structure

Above, the structure of lysenin assembly was described on the basis of AFM data and the crystal structure of lysenin pore. In this section, the assembly mechanism of lysenin into an hcp structure will be discussed. Although ordered assemblies of some PFTs were visualized by AFM **[29,32,33]**, the assembly pathway of PFTs into an ordered structure, reminiscent of two-dimensional crystals, has not been reported except for lysenin. Thus, lysenin can be a model toxin to understand the behavior of PFTs forming small oligomers. Since the final structure of lysenin assembly resembles a two-dimensional crystal, it should be appropriate to interpret its mechanism of assembly with the help of the information obtained from the crystallization pathways of other proteins.

The formation of two-dimensional crystals of some proteins, such as lysozyme, insulin, apoferritin, annexin V and HIV capsid protein, was visualized by AFM **[34-41]**. While lysozyme, insulin and apoferritin form multilayers, the crystals of annexin V and HIV capsid protein are made of a monomolecular layer at the solid-liquid interface. The general mechanism suggested for crystallization is nucleation, growth of crystal domains and their merging. The assembly of lysenin exhibits a similar mechanism after membrane binding and oligomerization **[13]**. The domains of close-packed lysenin oligomers forming on different regions of the membrane merge in a time interval shorter than a minute, resulting in the formation of a stable hexagonal two-dimensional crystal-like structure **(Figure 3)**.

A close look at the assembly pathway also revealed that lysenin oligomers reorganize via lateral diffusion during the growth of the crystal-like domains **[13]**. The fast reorganization of lysenin enables the formation of an hcp assembly with only a few defects. In the initial stages of assembling, there are both disordered and ordered assemblies of oligomers. The disordered assemblies are the diffusive regions in which the oligomers are randomly distributed. The ordered assemblies are either arrays or small domains of hcp oligomers. The randomly forming oligomers and arrays of oligomers are more susceptible to dissociation and reorganization than the close-packed oligomers. The randomly forming oligomers gradually diminish and the domains of close-packed oligomers grow larger in time, similar to Ostwald ripening. During the growth of domains, the domain edges manifest high dynamics because of the high line energy, resulting from the smaller number of interaction sites, and/or the misorientation of the oligomers **[42]**. The AFM images collected within a time interval of 0.15 s show the association and dissociation of oligomers at domain edges **(Figure 4)**. The average residence time of lysenin oligomers was found to be ~0.45 s. Using conventional AFMs, the incorporation of protein monomers or clusters into the crystal lattice can be tracked at high temporal resolution only along a single scan line, which is named the linescan technique **[35,36,38,39]**. This technique may provide a scan rate as high as 1 line/ms, however, the scanner drift can be a significant artifact for linescan imaging. Thus, employment of high-speed AFM is necessary for the visualization of protein dynamics at high spatio-temporal resolution.

2.3. Effect of molecular crowding on lysenin assembly

Although the existence of both stable hcp oligomers and dynamic oligomers during assembling of lysenin on SM/Chol (1/1) (mol/mol) bilayer was revealed by Yilmaz *et al.* **[13]**, their lateral diffusion was examined quantitatively in a recent study by Munguira *et al.* **[43]**. The authors employed a novel analysis methodology to analyze the high-speed AFM images

of the assembly of lysenin oligomers formed by preincubation on the SM/Chol (1/1) (mol/mol) membrane. Using this technique, they correlated the protein diffusion to the molecular environment. In this analysis technique, which provides very useful information on the dynamics of the oligomers and the domain characteristics, the time-dependent stability of lysenin oligomers was quantified by the calculation of variance and kurtosis. The analysis shows the coexistence of several diffusion regimes: the solid phase, which consists of stable hcp oligomers of lysenin, the liquid phase, where the oligomers freely diffuse, and the glassy phase, in which the oligomer mobility is restricted by immobile oligomers. The glassy phase was also categorized as sliding glass and fluid glass. The oligomers surrounding the solid phase were trapped for time scales up to minutes and named "sliding glass". The term "fluid glass" was used for the oligomers which were caged for periods shorter than 10 s. Additionally, the averaging of images revealed that a few oligomers in pore state were stuck because of interacting with the mica surface. These trapped oligomers affect the diffusion of the surrounding oligomers. The existence of stuck oligomers, which may cause some defects in the final close-packed structure, is a good proof of the possible effect of the mica substrate on the local membrane diffusion and the assembly structure. These findings may help to explain the disordered assemblies of lysenin oligomers observed on some regions of the membrane by Yilmaz *et al.* **[13]**.

2.4. Thermodynamic aspects of lysenin assembly

The hcp assembly of lysenin oligomers is thermodynamically stable after covering the entire membrane. The assembly pathway of lysenin consists of three steps: 1) lysenin binds the membrane via electrostatic attraction between its C-terminal domain and the phosphocholine headgroups of SM molecules **[1,20,21]**, 2) lysenin monomers diffuse rapidly along the membrane surface and oligomerize through the interaction between their C-terminal domains **[21]**, 3) lysenin oligomers reorganize on the membrane surface via rapid lateral diffusion to assemble into an hcp structure. Although lysenin strongly binds to SM, the fluidity of the liquid-ordered SM/Chol membrane facilitates the oligomerization of lysenin by enabling the fast lateral diffusion of the monomers on the membrane surface **[7]** and the assembling of oligomers into an hcp structure. The lipid membrane-mediated protein assembly yields a stable ordered structure, unlike most two-dimensional supramolecular architectures, which are constructed on solid surfaces via weak adsorbate-substrate interactions **[44]**.

The reaction enthalpy for binding of lysenin to SM/DOPC and SM/DOPC/Chol liposomes was measured to be between -3.6 to -4.4 kcal/mol SM (-18 to 26.4 kcal/mol lysenin) at 25 °C in previous studies **[7,45]**. Thus, the binding of lysenin to the membrane, which is the first step

in lysenin assembly, is likely enthalpy-driven, *i.e.*, the enthalpic contribution to the free energy change is higher than the unfavorable entropy of association **[46,47]**. In the second step, oligomerization of lysenin is promoted by its high concentration on the membrane surface and high lateral mobility. The fast oligomerization of lysenin can be ascribed to the attraction between the C-terminal domains of its membrane-bound monomers. This attractive interaction might be of hydrophobic origin, since the water molecules structuring around the hydrophilic domains lead to repulsion, which increases the energy barrier and accordingly slows down the association **[48-50]**. Besides the attraction between lysenin monomers, the contribution of entropy to the protein association should also be taken into consideration. Despite the restricted translational and rotational freedom, the increase in vibrational entropy favors the protein association **[51,52]**. Also, the entropy gain upon release of water molecules in the hydration shell of each monomer into the bulk water might further the oligomerization of lysenin. The hydration shell is structurally different than the bulk water **[53-56]**. It is mainly a monolayer of water molecules (~0.3 nm), which has a higher density and thus a lower mobility than the bulk water because of being structurized or restrained at the interface **[54,57,58]**. However, the thickness of the hydration layer may extend to four layers with the first layer being the most retarded due to the stronger hydrogen bonding **[59,60]**. Upon association of protein monomers, the release of water surrounding the protein leads to an increase in the entropy of the bulk solution. Vekilov *et al.* **[61,62]** reported that the entropy gain due to the disruption of the hydration layer is much larger than the entropy loss resulting from the immobilization of protein molecules within the crystal lattice. Thus, the main thermodynamic driving force for the crystallization of proteins was attributed to the maximization of the entropy of water. The same mechanism can be suggested for the third step of lysenin assembly, *i.e.*, the assembly of lysenin oligomers into an hcp structure, since most of the oligomers locally crystallized in the course of assembly at the expense of the decrease in their lateral motion.

3. Lysenin assembly on phase-separated membranes of SM

3.1. Selective binding of lysenin to SM-rich domains

Although lysenin specifically interacts with SM, biochemical analyses on model and cell membranes indicate that its binding to the membrane is dependent on the biophysical state of SM determined by the coexistence of other lipids in the membrane. The presence of glycolipids, such as glucosylceramide, galactosylceramide or gangliosides, in the same membrane dramatically reduces the binding of lysenin to the membrane **[45,63]**. This phenomenon is observed not only in model membranes, but also in cell membranes. In

polarized MDCK epithelial cells, apical membranes are highly enriched with glycolipids and only basolateral membranes are accessible for lysenin. Another example is mouse melanoma cell line and its mutants. Parental MEB4 cells that contain high amounts of glycolipids are resistant to lysenin, whereas mutant GM95 cells lacking glucosylceramide synthase, which is the enzyme necessary for the first step of glycolipid synthesis, are sensitive to the toxin. The revertant GM95 cell line, where glucosylceramide synthase gene is re-introduced, becomes resistant again. These results imply two possibilities: 1) sugar chains of glycolipids prevent the interaction between SM and lysenin due to steric hindrance, or 2) glycolipids change the distribution of SM in the membrane because both lipids are preferentially located in the same membrane microdomains called lipid rafts. Studies using model membranes support the latter possibility. Lysenin is capable of accessing to SM/DOPC liposomes, while it does not bind to SM/dipalmitoylphosphatidylcholine (DPPC) liposomes **[45]**. In the membrane, SM mixes well with DPPC, but not with DOPC, because the gel-to-liquid crystalline phase transition temperature of SM is almost the same as that of DPPC and much higher than that of DOPC. As a result, SM molecules form clusters in DOPC liposomes, whereas they are dispersed in DPPC liposomes **[64]**. Taken together, lysenin can recognize clustered SM, but not dispersed SM. The binding stoichiometry calculated from the isothermal titration calorimetry is one lysenin to five SM molecules, supporting the idea that lysenin binds to clustered SM **[45]**. Furthermore, fluorescent non-toxic truncated lysenin also preferentially recognizes clustered SM in model membranes as well as cell plasma membrane **[63]**.

The selective binding of lysenin to SM-rich domains was also studied using AFM. The localization of lysenin on SM-rich domains of phase-separated membranes was directly visualized by AFM imaging **[16,63,65]**. These results will be discussed in *Section 3.2*. In addition to AFM imaging, the findings from direct force measurement by AFM provided useful information about the strength of the lysenin-SM interaction and the nanomechanical properties of the membrane **[66]**. The force curves measured between an AFM tip conjugated with lysenin and the SM-including bilayers showed that lysenin interacts with SM-containing membranes only at high local concentrations of SM, *i.e.*, clustered SM. Attractive forces were observed for SM, SM/Chol bilayers and the phase-separated bilayers of SM. Lysenin did not bind SM/DPPC membrane because of SM being dispersed within the gel phase DPPC, as mentioned above. Thus, SM/DPPC membrane exhibited zero force. The comparison of the binding forces obtained for SM, SM/Chol membranes and the SM-rich domains in phase-separated membranes indicated that the strength of the attraction between lysenin and SM does not vary with lipid composition as long as SM forms clusters. However, the two-dimensional force mapping revealed the existence of additional attractive forces weaker

than those observed in the SM-rich domains surrounded by the DOPC-rich phase. These forces were exerted by small clusters of SM, which could not be resolved by AFM imaging, in the DOPC-rich phase. The detection of such small clusters of SM suggests that force mapping by AFM is a strong method to resolve the SM distribution at high precision. In addition to the chemical identity, the degree of membrane deformation was also obtained from the force curves. The mechanical deformation, resulting from the pull-off force during tip retraction, depended strongly on the lipid composition. For pure SM bilayer, which is in gel phase, the deformation was found to be minimum. The addition of 15% Chol or 50% DOPC to SM increased the membrane elasticity and accordingly the deformation.

3.2. Effect of phase coexistence on lysenin assembly

In the previous section, the affinity of lysenin to clustered SM was discussed. In this section, we will discuss the effect of phase coexistence on lysenin assembly and the membrane reorganization induced by lysenin. At phase boundary, line tension exists because of the deformations caused by the hydrophobic mismatch **[67,68]**. In addition, the lack of a stable hydration layer at the boundary **[69]** reduces the energy barrier for the adsorption of biomolecules. Because of these reasons, proteins and peptides may prefer to bind or localize at the phase boundary **[70-72]**. Equinatoxin II (EqII), which is another SM-binding PFT, initially binds the boundary between the liquid-ordered (Lo) and the liquid-disordered (Ld) phases before concentrating in the SM-poor Ld phase, as demonstrated by total internal reflection fluorescence imaging on droplet interface bilayers **[73]**.

Before explaining the assembly pathway of lysenin on a phase-separated membrane of SM and the effect of phase coexistence on its assembly, the different lipid-phase distribution of lysenin and EqII, the two SM-binding toxins, will be discussed. Both the confocal microscopy and AFM images show that lysenin and EqII prefer clustered and dispersed SM, respectively **[63]**. Apparently, EqII needs fewer SM molecules than lysenin to bind the membrane. The affinity of these two toxins to different membrane regions might also be resulting from the differences in their assembly pathway. Lysenin forms prepores before membrane insertion, whereas EqII oligomerizes after insertion of its N-terminal domain into the lipid bilayer **[74]**. Hence, EqII may need looser lipid packing, favoring the fast membrane insertion of single N-terminal domains and the addition of monomers into the inserted oligomeric assembly of EqII. As discussed in a recent review by Rojko and Anderluh **[30]**, the lipid headgroups in Ld phase are more exposed than those in Lo phase; hence, PFT binding can be enhanced in the fluid regions of the membrane. In addition, these regions may facilitate the pore formation by lowering the energetic barrier for the insertion of PFTs into the membrane. However, not only

the membrane fluidity, but the hydrophobic mismatch between the transmembrane region of PFT oligomers and the lipid bilayer plays an important role as well. Lysenin pores, having a long β-barrel, can be accommodated only in the thicker Lo phase. Briefly, the SM concentration, membrane fluidity and the membrane thickness should be the factors effective in the partitioning of lysenin and EqII in different regions of the membrane.

In the course of assembly of lysenin on SM/DOPC/Chol membrane, lysenin first assembles on the SM-rich Lo domains of SM/DOPC/Chol membrane **[16]**. It shows no apparent affinity to the phase boundary, in contrast to EqII, despite the lipid packing defects and the higher accessibility to SM headgroups at the boundary than on the Lo domains. After the full coverage of the SM-rich domains by oligomers, their hcp assembly gradually expands into the Ld phase and eventually covers the entire membrane. The full coverage of the membrane with an hcp assembly of lysenin oligomers denotes the complete mixing of Lo and Ld phases. The mechanism underlying the phase mixing was ascribed to the pore formation by lysenin. It is highly possible that the interactions between lipid molecules in the SM-rich Lo domains are interrupted during pore formation and subsequently the excess SM and Chol in the Lo domains are expelled into the DOPC-rich Ld phase. The excluded SM and Chol can form undetectably small clusters, facilitating the further binding of lysenin to the membrane after the full coverage of the Lo domains with oligomers. Thus, the gradual phase mixing leads to the enlargement of the hcp assembly. The mechanism of lysenin-induced membrane reorganization is illustrated in **Figure 5**. Phase mixing was also observed for other SM-binding toxins. Sticholysins I and II accumulate in the Ld phase of SM/DOPC/Chol membrane, similar to EqII, and induce phase mixing by membrane insertion **[75]**. Membrane rearrangement is likely to occur only in case of pore formation or membrane penetration. α-Hemolysin, which binds the phase boundary and concentrates in the Ld phase, does not cause any significant change in the lateral membrane organization because it does not insert into the membrane at the phase boundary and only partially spans the membrane in the Ld phase **[76]**. As a conclusion, the AFM observations for sticholysins and α-hemolysin support the mechanism suggested for the membrane reorganization induced by lysenin.

Although the phase boundary between SM-rich Lo domains and DOPC-rich Ld phase is not the concentration platform for lysenin, the behavior of lysenin can be different in the absence of Chol. AFM images recorded using a conventional AFM showed the localization of lysenin oligomers along the boundary between SM-rich and dilauroylphosphatidylcholine (DLPC)-rich phases in the absence of Chol **[65]**. Because of the high rigidity of SM-rich domains in the absence of Chol, the boundary may become more attractive for lysenin due to the lipid packing defects. Lysenin was not observed at the phase boundary between the

SM-rich and DLPC-rich phases in the presence of Chol. One reason might be the high lateral diffusion enabling the fast motion of lysenin from the boundary toward the center of the SM-rich Lo domains and thus preventing the accumulation of lysenin at the boundary. Similar phenomenon was observed for the partitioning of alkaline phosphatase on SM/DOPC and SM/DOPC/Chol membranes **[77]**. The Chol-dependent distribution was attributed to the variations in lateral diffusion and line tension. In case of lysenin, the concentration of SM at phase boundary should also have a pronounced effect on the affinity of lysenin to the boundary. The absence of lysenin oligomers at the phase boundary of Chol-containing membranes might imply the insufficient concentration of interfacial SM molecules. Hence, the Chol-dependent partitioning of lysenin can be a useful finding to probe the relative concentration of interfacial SM at different lipid compositions.

4. Functions of lysenin besides its well-known toxic action

4.1. Applications of lysenin in biology

Since the characterization of its SM-directed cytolytic effect, the full-length lysenin was proved to be useful in isolating lysenin-resistant mutant cells due to the defect of SM at the plasma membrane. These experiments were essential for the identification by the expression cloning method of the enzymatic activities responsible of the resistance against lysenin, such as the ceramide transfer protein (CERT) as the protein defective in the mutagenized CHO cells, LY-A **[78,79]**, and the SM synthase1 (SMS1) lacking in the SM-deficient mouse lymphoid cells **[80]**. The SM-specific toxicity of lysenin was also used to identify new inhibitors of SM metabolism by high-throughput microscopy screening **[81]**.

The addition of various tags such as maltose-binding protein (MBP), glutathione-S-transferase (GST), enhanced green fluorescent protein (EGFP), Dronpa, mCherry to the N terminus of the non-toxic (NT)-lysenin (fragment 161-297) did not change its binding specificity and these labeled NT-lysenin have been used to observe SM distribution by confocal and super resolution microscopy **[5,8,63,82-84]**. GST-tagged NT-lysenin demonstrated the accumulation of SM in the lysosomes of fixed and permeabilized fibroblasts from patients with Niemann Pick type A disease deficient in lysosomal acid sphingomyelinase **[8]**. SM-rich domains with an average radius of 124 nm were observed by photoactivated localization microscopy (PALM) analysis in living HeLa cells stained with photoswitchable fluorescent Dronpa-NT-Lysenin **[82]**. In addition, phosphatidylinositol bisphosphate (PIP2) clusters labeled with Dronpa-PH domain in the inner leaflet of the plasma membrane of LLC-PK1 cells were localized just beneath the SM clusters labeled by Alexa 647-lysenin in the outer leaflet. Depletion of SM by sphingomyelinase treatment dispersed PIP2 and inhibited

the recruitment of the small GTPase RhoA to the cleavage furrow, leading to abnormal cytokinesis **[83]**.

In addition to fluorescence microscopy, lysenin can be used in immunoelectron microscopy analysis. Using SDS-digested freeze-fracture replica labeling (SDS-FRL) immunoelectron microscopy with MBP-lysenin, Murate *et al.* **[85]** revealed the presence of SM domains and analyzed the transbilayer SM distribution in the plasma membrane. SM was found exclusively in the outer leaflet of human red blood cells, whereas about 12% of SM were distributed in the inner leaflet of human skin fibroblasts. In addition, SM domains with a radius of 60-180 nm were detected in the inner leaflet, whereas SM domains with an average radius of 36 nm were in the outer leaflet. Furthermore full-length lysenin and its tagged non-toxic fragments are often used to verify the efficiency of sphingomyelinase treatment, the knockdown or the overexpression of SMS in various cells or in model membranes **[86,87]**.

Recently He *et al.* **[88]** used nanoscale secondary ion mass spectrometry (nanoSIMS) imaging with 15N-labeled lysenin in combination with 15N-labeled Chol-binding proteins (perfringolysin O and its domain D4 ALO-D4) to visualize SM-rich and Chol-rich domains in the plasma membrane of CHO cells. Their results revealed that Chol and SM are not distributed evenly, but are enriched on the surface of microvilli. In addition, the distribution of Chol and SM were found similar (but not fully identical) in contrast to the results of Fritz *et al.* **[89]** that used nanoSIMS imaging with 15N-labeled sphingolipid precursors and 18O-labeled Chol to visualize sphingolipid-rich and Chol-rich domains. While sphingolipids were unevenly distributed forming domains with a mean diameter of 200 nm, Chol was evenly distributed in the plasma membrane of 3T3 fibroblasts.

4.2. Possible applications of lysenin in biotechnology

PFT pores can be functionalized to be employed as biosensors. The change in the ionic current passing through the pores under an applied potential can provide information about the concentration and the identity of the analyte. The detection of metal ions, organic molecules and macromolecules by α-hemolysin pores was reviewed by Bayley *et al.* **[90-92]**.

The sensitivity of the lysenin pore to metal and organic cations was studied by electro-physiological measurements to shed light on the pore activity **[93-101]**. Single-channel experiments showed that lysenin pores incorporated into asolectin bilayers function as voltage-gated channels with low ion selectivity **[93]**. Further investigations revealed that salt concentration and pH highly affect the gating of lysenin pores, indicating that the gating mechanism is governed by the electrostatic interactions **[94]**. The ionic transport increases as the concentration of monovalent metal cations is heightened, whereas multivalent metal

cations induce partial or full closing of the lysenin channels **[95]**. Similar to multivalent metal cations, cationic polymers also prompt the current blockage because of being trapped inside the channel **[98]**. The lysenin pores switch from open to partially closed or closed states due to the conformational changes induced by multivalent metal cations and highly charged organic cations. The sensitivity of the lysenin pore to DNA was also examined **[21,102]** and the effect of DNA on the single channel current indicated that lysenin pore may become a candidate nanopore for DNA detection in the future. Considering that the PFT pores have received attention especially in DNA sequencing **[103]**, further examination and improvement of the properties of the lysenin pore are necessary. Advantages of lysenin in the development of PFT nanopores as sensors are its stability in pore state and tendency to form complete oligomers. Because the arc-shaped proteolipidic pores are noisier and have lower ionic conductivity than ring-shaped pores **[104]**, the high ratio of complete oligomers of lysenin to arcs may provide reproducible and high pore activity.

In addition to biosensing, the lysenin pore may have other potential future applications such as drug delivery, cancer treatment and development of biobatteries **[105,106]**. AFM visualization of the voltage-dependent gating of the lysenin pore and its interaction with organic and biological molecules would help to unravel its possible functions in nanobiotechnology and nanomedicine.

5. Conclusions

Due to the better characterization of its molecular mechanism of action, the SM-specific protein, lysenin (and its derivatives) has attracted increasing attention not only as a specific tool to visualize the distribution and dynamics of SM in model and cell membranes in various patho-physiological conditions, but also in a more general approach, as a model of PFT assembly and PFT-induced membrane reorganization for high resolution techniques.

AFM imaging demonstrated the assembly pathway of lysenin on both homogenous and phase-separated membranes of SM. Although the hcp structure formed by lysenin oligomers on SM-containing liposomes was visualized in earlier studies using TEM, the mechanism of assembly was not known. The high-speed AFM technique, providing high temporal and spatial resolution, allowed the examination of the dynamic processes occurring during the assembly of lysenin on model membranes. This review summarizes all these findings together with the data obtained by biochemical and other biophysical techniques. Two factors play significant roles in the assembly of lysenin. These are the local concentration of SM and the presence of Chol. It is well known that lysenin binds to clustered SM, and the presence of Chol facilitates the oligomerization of lysenin. The high lateral diffusion along the SM/Chol membrane allows

the hexagonal close packing of lysenin oligomers. Although the oligomerization of lysenin could not be tracked, the assembly of lysenin oligomers into an hcp structure could be successfully followed using high-speed AFM. The effect of phase coexistence on lysenin assembly was also studied using the same technique. A careful examination of the time-lapse AFM images revealed that pore formation in SM-rich domains induces phase mixing. Without high-speed scanning, it would have been difficult to determine the mechanism of membrane reorganization. Interestingly, lysenin oligomers were not detected at the phase boundary during the early stages of assembly. However, in another study they were found to localize at the phase boundary in the absence of Chol, possibly due to the higher interfacial concentration of SM and the higher line energy. Since the distribution of lysenin along the SM-rich domains may show some differences depending on the lipid composition, performing the experiments of lysenin assembly on cell membranes using AFM will comprehend the toxic action of lysenin. Unlike model membranes, the assembly of lysenin and other PFTs on cell membranes has not been studied at high resolution. The recent development of long-tip high-speed AFM **[107]** may enable the examination of the PFT assembly on cell membranes at high spatiotemporal resolution. In addition to living cell membranes, plasma membrane fragments such as giant plasma membrane vesicles **[108,109]** will be useful to study the toxin assembly for a complex system. Upon fusion of these vesicles, flat membrane patches may form on the solid substrate, allowing the high-resolution imaging. While working with cell membranes, another point that should be considered is the identification of the target molecule within a crowded environment. For this purpose, force measurements using anti-lysenin antibody can be performed for the detection of lysenin on the cell membrane. These techniques together with other techniques such as *in situ* fluorescent measurement will provide further information on the molecular mechanisms of lysenin assembly.

Acknowledgements. This work was supported by the Integrated Lipidology Program of RIKEN and Grants-in-Aid for Scientific Research 25293015 (to TK) from the Ministry of Education, Culture, Sports, Science and Technology of Japan.

References

[1] L. De Colibus, A.F.-P. Sonnen, K.J. Morris, C.A. Siebert, P. Abrusci, J. Plitzko, V. Hodnik, M. Leippe, E. Volpi, G. Anderluh, R.J.C. Gilbert, Structures of lysenin reveal a shared evolutionary origin for pore-forming proteins and its mode of sphingomyelin recognition, Structure 20 (2012) 1498-1507.

[2] Y. Sekizawa, T. Hagiwara, T. Nakajima, H. Kobayashi, A novel protein, lysenin, that

causes contraction of the isolated rat aorta: its purification from the coelomic fluid of the earthworm, *Eisenia foetida*, Biomed. Res. 17 (1996) 197-203.

[3] A. Yamaji, Y. Sekizawa, K. Emoto, H. Sakuraba, K. Inoue, H. Kobayashi, M. Umeda, Lysenin, a novel sphingomyelin-specific binding protein, J. Biol. Chem. 273 (1998) 5300-5306.

[4] Y. Sekizawa, T. Kubo, H. Kobayashi, T. Nakajima, S. Natori, Molecular cloning of cDNA for lysenin, a novel protein in the earthworm *Eisenia foetida* that causes contraction of rat vascular smooth muscle, Gene 191 (1997) 97-102.

[5] E. Kiyokawa, A. Makino, K. Ishii, N. Otsuka, A. Yamaji-Hasegawa, T. Kobayashi, Recognition of sphingomyelin by lysenin and lysenin-related proteins, Biochemistry 43 (2004) 9766-9773.

[6] A. Yamaji-Hasegawa, A. Makino, T. Baba, Y. Senoh, H. Kimura-Suda, S.B. Sato, N. Terada, S. Ohno, E. Kiyokawa, M. Umeda, T. Kobayashi, Oligomerization and pore formation of a sphingomyelin-specific toxin, lysenin, J. Biol. Chem. 278 (2003) 22762-22770.

[7] R. Ishitsuka, T. Kobayashi, Cholesterol and lipid/protein ratio control the oligomerization of a sphingomyelin-specific toxin, lysenin, Biochemistry 46 (2007) 1495-1502.

[8] E. Kiyokawa, T. Baba, N. Otsuka, A. Makino, S. Ohno, T. Kobayashi, Spatial and functional heterogeneity of sphingolipid-rich membrane domains, J. Biol. Chem. 280 (2005) 24072-24084.

[9] N. Yilmaz, T. Kobayashi, Assemblies of pore-forming toxins visualized by atomic force microscopy, Biochim. Biophys. Acta 1858 (2016) 500-511.

[10] A.W. Hodel, C. Leung, N.V. Dudkina, H.R. Saibil, B.W. Hoogenboom, Atomic force microscopy of membrane pore formation by cholesterol-dependent cytolysins, Curr. Opin. Struct. Biol. 39 (2016) 8-15.

[11] T. Ando, N. Kodera, E. Takai, D. Maruyama, K. Saito, A. Toda, A high-speed atomic force microscope for studying biological macromolecules, Proc. Natl. Acad. Sci. USA 98 (2001) 12468-12472.

[12] T. Ando, T. Uchihashi, S. Scheuring, Filming biomolecular processes by high-speed atomic force microscopy, Chem. Rev. 114 (2014) 3120-3188.

[13] N. Yilmaz, T. Yamada, P. Greimel, T. Uchihashi, T. Ando, T. Kobayashi, Real-time visualization of assembling of a sphingomyelin–specific toxin on planar lipid membranes, Biophys. J. 105 (2013) 1397-1405.

[14] R.J.C. Gilbert, Pore-forming toxins, Cell. Mol. Life Sci. 59 (2002) 832-844.

[15] H. Bayley, L. Jayasinghe, M. Wallace, Prepore for a breakthrough, Nat. Struct. Mol. Biol. 12 (2005) 385-386.

[16] N. Yilmaz, T. Kobayashi, Visualization of lipid membrane reorganization induced by a pore-forming toxin using high-speed atomic force microscopy, ACS Nano 9 (2015) 7960-7967.

[17] D.M. Czajkowsky, E.M. Hotze, Z. Shao, R.K. Tweten, Vertical collapse of a cytolysin prepore moves its transmembrane β-hairpins to the membrane, EMBO J. 23 (2004) 3206-3215.

[18] C. Leung, N.V. Dudkina, N. Lukoyanova, A.W. Hodel, I. Farabella, A.P. Pandurangan, N. Jahan, M.P. Damaso, D. Osmanović, C.F. Reboul, M.A. Dunstone, P.W. Andrew, R. Lonnen, M. Topf, H.R. Saibil, B.W. Hoogenboom, Stepwise visualization of membrane pore formation by suilysin, a bacterial cholesterol-dependent cytolysin, eLife 3 (2014), e04247.

[19] M. Podobnik, M. Marchioretto, M. Zanetti, A. Bavdek, M. Kisovec, M.M. Cajnko, L. Lunelli, M.D. Serra, G. Anderluh, Plasticity of lysteriolysin O pores and its regulation by pH and unique histidine, Sci. Rep. 5 (2015) 9623.

[20] M. Bokori-Brown, T.G. Martin, C.E. Naylor, A.K. Basak, R.W. Titball, C.G. Savva, Cryo-EM structure of lysenin pore elucidates membrane insertion by an aerolysin family protein, Nat. Commun. 7 (2016) 11293.

[21] M. Podobnik, P. Savory, N. Rojko, M. Kisovec, N. Wood, R. Hambley, J. Pugh, E.J. Wallace, L. McNeill, M. Bruce, I. Liko, T.M. Allison, S. Mehmood, N. Yilmaz, T. Kobayashi, R.J.C. Gilbert, C.V. Robinson, L. Jayasinghe, G. Anderluh, Crystal structure of an invertebrate cytolysin pore reveals unique properties and mechanism of assembly, Nat. Commun. 7 (2016) 11598.

[22] L. Song, M.R. Hobaugh, C. Shustak, S. Cheley, H. Bayley, J.E. Gouaux, Structure of staphylococcal α-hemolysin, a heptameric transmembrane pore, Science 274 (1996) 1859-1866.

[23] K. Yamashita, Y. Kawai, Y. Tanaka, N. Hirano, J. Kaneko, N. Tomita, M. Ohta, Y. Kamio, M. Yao, I. Tanaka, Crystal structure of the octameric pore of staphylococcal γ-hemolysin reveals the β-barrel pore formation mechanism by two components, Proc. Natl. Acad. Sci. USA 108 (2011) 17314-17319.

[24] M.T. Degiacomi, I. Iacovache, L. Pernot, M. Chami, M. Kudryashev, H. Stahlberg, F.G. van der Goot, M.D. Peraro, Molecular assembly of the aerolysin pore reveals a swirling membrane-insertion mechanism, Nat. Chem. Biol. 9 (2013) 623-629.

[25] R.J.C. Gilbert, M. Mikelj, M. Dalla Serra, C.J. Froelich, G. Anderluh, Effects of MACPF/CDC proteins on lipid membranes, Cell. Mol. Life Sci. 70 (2013) 2083-2098.

[26] R.J.C. Gilbert, M. Dalla Serra, C.J. Froelich, M.I. Wallace, G. Anderluh, Membrane pore formation at protein-lipid interfaces, Trends Biochem. Sci. 39 (2014) 510-516.

[27] J.R. Thompson, B. Cronin, H. Bayley, M.I. Wallace, Rapid assembly of a multimeric membrane protein pore, Biophys. J. 101 (2011) 2679-2683.

[28] E.M. Hotze, E. Wilson-Kubalek, A.J. Farrand, L. Bentsen, M.W. Parker, A.E. Johnson, R.K. Tweten, Monomer-monomer interactions propagate structural transitions necessary for pore formation by the cholesterol-dependent cytolysins, J. Biol. Chem. 287 (2012) 24534-24543.

[29] D.M. Czajkowsky, S. Sheng, Z. Shao, Staphylococcal α-hemolysin can form hexamers in phospholipid bilayers, J. Mol. Biol. 276 (1998) 325-330.

[30] N. Rojko, G. Anderluh, How lipid membranes affect pore forming toxin activity, Acc. Chem. Res. 48 (2015) 3073-3079.

[31] A.A. Lee, M.J. Senior, M.I. Wallace, T.E. Woolley, I.M. Griffiths, Dissecting the self-assembly kinetics of multimeric pore-forming toxins, J. R. Soc. Interface 13 (2016) 20150762.

[32] J. Mou, J. Yang, Z. Shao, Atomic force microscopy of cholera toxin B-oligomers bound to bilayers of biologically relevant lipids, J. Mol. Biol. 248 (1995) 507-512.

[33] D.M. Czajkowsky, H. Iwamoto, T.L. Cover, Z. Shao, The vacuolating toxin from *Helicobacter pylori* forms hexameric pores in lipid bilayers at low pH, Proc. Natl. Acad. Sci. U.S.A. 96 (1999) 2001-2006.

[34] S.D. Durbin, W.E. Carison, Lysozyme crystal growth studied by atomic force microscopy, J. Cryst. Growth 122 (1992) 71-79.

[35] H. Li, A. Nadarajah, M.L. Pusey, Determining the molecular-growth mechanisms of protein crystal faces by atomic force microscopy, Acta Crystallogr. D55 (1999) 1036-1045.

[36] M. Wiechmann, O. Enders, C. Zeilinger, H.-A. Kolb, Analysis of protein crystal growth at molecular resolution by atomic force microscopy, Ultramicroscopy 86 (2001) 159-166.

[37] C.M. Yip, M.D. Ward, Atomic force microscopy of insulin single crystals: Direct visualization of molecules and crystal growth, Biophys. J. 71 (1996) 1071-1078.

[38] D.K. Georgiou, P.G. Vekilov, A fast response mechanism for insulin storage in crystals may involve kink generation by association of 2D clusters, Proc. Natl. Acad. Sci. USA 103 (2006) 1681-1686.

[39] S.-T. Yau, B.R. Thomas, P.G. Vekilov, Real time *in situ* monitoring of apoferritin crystallization and defect formation with molecular resolution, J. Cryst. Growth 232 (2001) 188-194.

[40] I. Reviakine, W. Bergsma-Schutter, A. Brisson, Growth of protein 2-D crystals on supported planar lipid bilayers imaged *in situ* by AFM, J. of Struct. Biol. 121 (1998) 356-361.

[41] A. Valbuena, M.G. Mateu, Kinetics of surface-driven self-assembly and fatigue-induced

disassembly of a virus-based nanocoating, Biophys. J. 112 (2017) 663-673.

[42] A. Lomakin, N. Asherie, G.B. Benedek, Aeolotopic interactions of globular proteins, Proc. Natl. Acad. Sci. USA 96 (1999) 9465-9468.

[43] I. Munguira, I. Casuso, H. Takahashi, F. Rico, A. Miyagi, M. Chami, S. Scheuring, Glasslike membrane protein diffusion in a crowded membrane, ACS Nano 10 (2016) 2584-2590.

[44] S. Uemura, R. Tanoue, N. Yilmaz, A. Ohira, M. Kunitake, Molecular dynamics in two-dimensional supramolecular systems observed by STM, Materials 3 (2010) 4252-4276.

[45] R. Ishitsuka, A. Yamaji-Hasegawa, A. Makino, Y. Hirabayashi, T. Kobayashi, A lipid-specific toxin reveals heterogeneity of sphingomyelin-containing membranes, Biophys. J. 86 (2004) 296-307.

[46] N. Ben-Tal, B. Honig, C.K. Bagdassarian, A. Ben-Shaul, Association entropy in adsorption processes, Biophys. J. 79 (2000) 1180-1187.

[47] J. Seelig, Thermodynamics of lipid–peptide interactions, Biochim. Biophys. Acta 1666 (2004) 40-50.

[48] D.N. Petsev, B.R. Thomas, S.-T. Yau, P.G. Vekilov, Interactions and aggregation of apoferritin molecules in solution: Effects of added electrolytes, Biophys. J. 78 (2000) 2060-2069.

[49] D.N. Petsev, B.R. Thomas, S.-T. Yau, D. Tsekova, C. Nanev, W.W. Wilson, P.G. Vekilov, Temperature-independent solubility and interactions between apoferritin monomers and dimers in solution, J. Cryst. Growth 232 (2001) 21-29.

[50] J.J. Valle-Delgado, J.A. Molina-Bolivar, F. Galisteo-Gonzalez, M.J. Galvez-Ruiz, A. Feiler, M.W. Rutland, Existence of hydration forces in the interaction between apoferritin molecules adsorbed on silica surfaces, Langmuir 21 (2005) 9544-9554.

[51] B. Tidor, M. Karplus, The contribution of vibrational entropy to molecular association: The dimerization of insulin, J. Mol. Biol. 238 (1994) 405-414.

[52] A. Tamura, P.L. Privalov, The entropy cost of protein association, J. Mol. Biol. 273 (1997) 1048-1060.

[53] J. Israelachvili, H. Wennerstrom, Role of hydration and water structure in biological and colloidal interactions, Nature 379 (1996) 219-225.

[54] D.I. Svergun, S. Richard, M.H.J. Koch, Z. Sayers, S. Kuprin, G. Zaccai, Protein hydration in solution: Experimental observation by x-ray and neutron scattering, Proc. Natl. Acad. Sci. USA 95 (1998) 2267-2272.

[55] B. Bagchi, Water dynamics in the hydration layer around proteins and micelles, Chem. Rev. 105 (2005) 3197-3219.

[56] N. Bhattacharjee, P. Biswas, Structure of hydration water in proteins: A comparison of molecular dynamics simulations and database analysis, Biophys. Chem. 158 (2011) 73-80.

[57] K. Yokoyama, T. Kamei, H. Minami, M. Suzuki, Hydration study of globular proteins by microwave dielectric spectroscopy, J. Phys. Chem. B 105 (2001) 12622-12627.

[58] L. Biedermannova, B. Schneider, Hydration of proteins and nucleic acids: Advances in experiment and theory. A review, Biochim. Biophys. Acta 1860 (2016) 1821-1835.

[59] R. Ghosh, S. Banerjee, M. Hazra, S. Roy, B. Bagchi, Sensitivity of polarization fluctuations to the nature of protein-water interactions: Study of biological water in four different protein-water systems, J. Chem. Phys. 141 (2014) 22D531:1-11.

[60] K. Shiraga, Y. Ogawa, N. Kondo, Hydrogen bond network of water around protein investigated with terahertz and infrared spectroscopy, Biophys. J. 111 (2016) 2629-2641.

[61] P.G. Vekilov, A.R. Feeling-Taylor, D.N. Petsev, O. Galkin, R.L. Nagel, R.E. Hirsch, Intermolecular interactions, nucleation, and thermodynamics of crystallization of hemoglobin C, Biophys. J. 83 (2002) 1147-1156.

[62] P.G. Vekilov, What determines the rate of growth of crystals from solution? Cryst. Growth Des. 7 (2007) 2796-2810.

[63] A. Makino, M. Abe, M. Murate, T. Inaba, N. Yilmaz, F. Hullin-Matsuda, T. Kishimoto, N.L. Schieber, T. Taguchi, H. Arai, G. Anderluh, R.G. Parton, T. Kobayashi, Visualization of the heterogeneous membrane distribution of sphingomyelin associated with cytokinesis, cell polarity, and sphingolipidosis, FASEB J. 29 (2015) 477-493.

[64] K. Shirota, K. Yagi, T. Inaba, P.-C. Li, M. Murata, Y. Sugita, T. Kobayashi, Detection of sphingomyelin clusters by raman spectroscopy, Biophys. J. 111 (2016) 999-1007.

[65] H. Shogomori, A. Makino, N. Yilmaz, M. Abe, T. Yamada, T. Kobayashi, Cholesterol alters membrane distribution of sphingomyelin-binding toxin, Unpublished results.

[66] T. Wang, H. Shogomori, M. Hara, T. Yamada, T. Kobayashi, Nanomechanical recognition of sphingomyelin-rich membrane domains by atomic force microscopy, Biochemistry 51 (2012) 74-82.

[67] T.R. Galimzyanov, R.J. Molotkovsky, S.A. Akimov, Line tension and structure of raft boundary calculated from bending, tilt, and lateral compression/stretching, Biol. Membrany 28 (2011) 415-422.

[68] D.W. Lee, Y. Min, P. Dhar, A. Ramachandran, J.N. Israelachvili, J.A. Zasadzinski, Relating domain size distribution to line tension and molecular dipole density in model cytoplasmic myelin lipid monolayers, Proc. Natl. Acad. Sci. USA 108 (2011) 9425-9430.

[69] K.H. Sheikh, S.P. Jarvis, Crystalline hydration structure at the membrane-fluid interface of model lipid rafts indicates a highly reactive boundary region, J. Am. Chem. Soc. 133 (2011)

18296-18303.

[70] C. Nicolini, J. Baranski, S. Schlummer, J. Palomo, M. Lumbierres-Burgues, M. Kahms, J. Kuhlmann, S. Sanchez, E. Gratton, H. Waldmann, R. Winter, Visualizing association of N-Ras in lipid microdomains: Influence of domain structure and interfacial adsorption, J. Am. Chem. Soc. 128 (2006) 192-201.

[71] A.J. Garcia-Saez, S. Chiantia, J. Salgado, P. Schwille, Pore formation by a Bax-derived peptide: Effect on the line tension of the membrane probed by AFM, Biophys. J. 93 (2007) 103-112.

[72] S.-T. Yang, V. Kiessling, L.K. Tamm, Line tension at lipid phase boundaries as driving force for HIV fusion peptide-mediated fusion, Nat. Commun. 7 (2016) 11401:1-9.

[73] N. Rojko, B. Cronin, J.S.H. Danial, M.A.B. Baker, G. Anderluh, M.I. Wallace, Imaging the lipid-phase-dependent pore formation of equinatoxin II in droplet interface bilayers, Biophys. J. 106 (2014) 1-8.

[74] N. Rojko, K.C. Kristan, G. Viero, E. Zerovnik, P. Macek, M.D. Serra, G. Anderluh, Membrane damage by an α-helical pore-forming protein, equinatoxin II, proceeds through a succession of ordered steps, J. Biol. Chem. 288 (2013) 23704-23715.

[75] U. Ros, M.A. Edwards, R.F. Epand, M.E. Lanio, S. Schreier, C.M. Yip, C. Alvarez, R.M. Epand, The sticholysin family of pore-forming toxins induces the mixing of lipids in membrane domains, Biochim. Biophys. Acta 1828 (2013) 2757-2762.

[76] S.M. Mate, R.F. Vazquez, V.S. Herlax, M.A. Daza Millone, M.L. Fanani, B.Maggio, M.E. Vela, L.S. Bakas, Boundary region between coexisting lipid phases as initial binding sites for Escherichia coli alpha-hemolysin: A real-time study, Biochim. Biophys. Acta 1838 (2014) 1832-1841.

[77] P.-E. Milhiet, M.-C. Giocondi, O. Baghdadi, F. Ronzon, B. Roux, C. Le Grimellec, Spontaneous insertion and partitioning of alkaline phosphatase into model lipid rafts, EMBO Rep. 3 (2002) 485-490.

[78] K. Hanada, T. Hara, M. Fukasawa, A. Yamaji, M. Umeda, M. Nishijima, Mammalian cell mutants resistant to a sphingomyelin-directed cytolysin, J. Biol. Chem. 273 (1998) 33787-33794.

[79] K. Hanada, K. Kumagai, S. Yasuda, Y. Miura, M. Kawano, M. Fukasawa, M. Nishijima, Molecular machinery for non-vesicular trafficking of ceramide, Nature 426 (2003) 803-809.

[80] S. Yamaoka, M. Miyaji, T. Kitano, H. Umehara, T. Okazaki, Expression cloning of a human cDNA restoring sphingomyelin synthesis and cell growth in sphingomyelin synthase-defective lymphoid cells, J. Biol. Chem. 279 (2004) 18688-18693.

[81] F. Hullin-Matsuda, N. Tomishige, S. Sakai, R. Ishitsuka, K. Ishii, A. Makino, P. Greimel,

M. Abe, E.L. Laviad, M. Lagarde, H. Vidal, T. Saito, H. Osada, K. Hanada, A.H. Futerman, T. Kobayashi, Limonoid compounds inhibit sphingomyelin biosynthesis by preventing CERT protein-dependent extraction of ceramides from the endoplasmic reticulum, J. Biol. Chem. 287 (2012) 24397-24411.

[82] H. Mizuno, M. Abe, P. Dedecker, A. Makino, S. Rocha, Y. Ohno-Iwashita, J. Hofkens, T. Kobayashi, A. Miyawaki, Fluorescent probes for superresolution imaging of lipid domains on the plasma membrane, Chem. Sci. 2 (2011) 1548-1553.

[83] M. Abe, A. Makino, F. Hullin-Matsuda, K. Kamijo, Y. Ohno-Iwashita, K. Hanada, H. Mizuno, A. Miyawaki, T. Kobayashi, A Role for sphingomyelin-rich lipid domains in the accumulation of phosphatidylinositol-4,5-bisphosphate to the cleavage furrow during cytokinesis, Mol. Cell. Biol. 32 (2012) 1396-1407.

[84] M. Carquin, H. Pollet, M. Veiga-da-Cunha, A. Cominelli, P. Van Der Smissen, F. N'kuli, H. Emonard, P. Henriet, H. Mizuno, P.J. Courtoy, D. Tyteca, Endogenous sphingomyelin segregates into submicrometric domains in the living erythrocyte membrane, J. Lipid Res. 55 (2014) 1331-1342.

[85] M. Murate, M. Abe, K. Kasahara, K. Iwabuchi, M. Umeda, T. Kobayashi, Transbilayer distribution of lipids at nano scale, J. Cell Sci. 128 (2015) 1627-1638.

[86] Z. Li, T.K. Hailemariam, H. Zhou, Y. Li, D.C. Duckworth, D.A. Peake, Y. Zhang, M.-S. Kuo, G. Cao, X.-C. Jiang, Inhibition of sphingomyelin synthase (SMS) affects intracellular sphingomyelin accumulation and plasma membrane lipid organization, BBA-Mol. Cell Biol. L. 1771 (2007) 1186-1194.

[87] T. Ding, Z. Li, T. Hailemariam, S. Mukherjee, F.R. Maxfield, M.-P. Wu, X.-C. Jiang, SMS overexpression and knockdown: impact on cellular sphingomyelin and diacylglycerol metabolism, and cell apoptosis, J. Lipid Res. 49 (2008) 376-385.

[88] C. He, X. Hu, R.S. Jung, T.A. Weston, N.P. Sandoval, P. Tontonoz, M.R. Kilburn, L.G. Fong, S.G. Young, H. Jiang, High-resolution imaging and quantification of plasma membrane cholesterol by NanoSIMS, Proc. Natl. Acad. Sci. USA 114 (2017) 2000-2005.

[89] J.F. Frisz, H.A. Klitzing, K. Lou, I.D. Hutcheon, P.K. Weber, J. Zimmerberg, M.L. Kraft, Sphingolipid domains in the plasma membranes of fibroblasts are not enriched with cholesterol, J. Biol. Chem. 288 (2013) 16855-16861.

[90] H. Bayley, O. Braha, L.-Q. Gu, Stochastic sensing with protein pores, Adv. Mater. 12 (2000) 139-142.

[91] H. Bayley, P.S. Cremer, Stochastic sensors inspired by biology, Nature 413 (2001) 226-230.

[92] H. Bayley, Sequencing single molecules of DNA, Curr. Opin. Chem. Biol. 10 (2006)

628-637.

[93] T. Ide, T. Aoki, Y. Takeuchi, T. Yanagida, Lysenin forms a voltage-dependent channel in artificial lipid bilayer membranes, Biochem. Biophys. Res. Commun. 346 (2006) 288-292.

[94] D. Fologea, E. Krueger, R. Lee, M. Naglak, Y. Mazur, R. Henry, G. Salamo, Controlled gating of lysenin pores, Biophys. Chem. 146 (2010) 25-29.

[95] D. Fologea, E. Krueger, R. Al Faori, R. Lee, Y.I. Mazur, R. Henry, M. Arnold, G.J. Salamo, Multivalent ions control the transport through lysenin channels, Biophys. Chem. 152 (2010) 40-45.

[96] D. Fologea, R. Al Faori, E. Krueger, Y.I. Mazur, M. Kern, M. Williams, A. Mortazavi, R. Henry, G.J. Salamo, Potential analytical applications of lysenin channels for detection of multivalent ions, Anal. Bioanal. Chem. 401 (2011) 1871-1879.

[97] D. Fologea, E. Krueger, Y.I. Mazur, C. Stith, Y. Okuyama, R. Henry, G.J. Salamo, Bi-stability, hysteresis, and memory of voltage-gated lysenin channels, Biochim. Biophys. Acta 1808 (2011) 2933-2939.

[98] D. Fologea, E. Krueger, S. Rossland, S. Bryant, W. Foss, T. Clark, Cationic polymers inhibit the conductance of lysenin channels, Scientific World J. 2013 (2013) 1-8.

[99] E. Krueger, R. Al Faouri, D. Fologea, R. Henry, D. Straub, G. Salamo, A model for the hysteresis observed in gating of lysenin channels, Biophys. Chem. 184 (2013) 126-130.

[100] E. Krueger, S. Bryant, N. Shrestha, T. Clark, C. Hanna, D. Pink, D. Fologea, Intramembrane congestion effects on lysenin channel voltage−induced gating, Eur. Biophys. J. 45 (2016) 187-194.

[101] S. Bryant, N. Shrestha, P. Carnig, S. Kosydar, P. Belzeski, C. Hanna, D. Fologea, Purinergic control of lysenin's transport and voltage-gating properties, Purinergic Signal. 12 (2016) 549-559.

[102] T. Aoki, M. Hirano, Y. Takeuchi, T. Kobayashi, T. Yanagida, T. Ide, Single channel properties of lysenin measured in artificial lipid bilayers and their applications to biomolecule detection, Proc. Jpn. Acad., Ser. B 86 (2010) 920-925.

[103] M. Ayub, H. Bayley, Engineered transmembrane pores, Curr. Opin. Chem. Biol. 34 (2016) 117-126.

[104] M. Marchioretto, M. Podobnik, M.D. Serra, G. Anderluh, What planar lipid membranes tell us about the pore-forming activity of cholesterol-dependent cytolysins, Biophys. Chem. 182 (2013) 64-70.

[105] S. Majd, E.C. Yusko, Y.N. Billeh, M.X. Macrae, J. Yang, M. Mayer, Applications of biological pores in nanomedicine, sensing, and nanoelectronics, Curr. Opin. Biotechnol. 21 (2010) 439-476.

[106] P.A. Gurnev, E.M. Nestorovich, Channel-forming bacterial toxins in biosensing and macromolecule delivery, Toxins 6 (2014) 2483-2540.

[107] M. Shibata, T. Uchihashi, T. Ando, R. Yasuda, Long-tip high-speed atomic force microscopy for nanometer-scale imaging in live cells, Sci. Rep. 5 (2014) 8724:1-7.

[108] T. Baumgart, A.T. Hammond, P. Sengupta, S.T. Hess, D.A. Holowka, B.A. Baird, W. Webb, Large-scale fluid/fluid phase separation of proteins and lipids in giant plasma membrane vesicles, Proc. Natl. Acad. Sci. USA 104 (2007) 3165-3170.

[109] K.R. Levental, I. Levental, Giant plasma membrane vesicles: models for understanding membrane organization, Curr. Top. Membr. 75 (2015) 25-57.

Figure Legends

Figure 1. Yilmaz

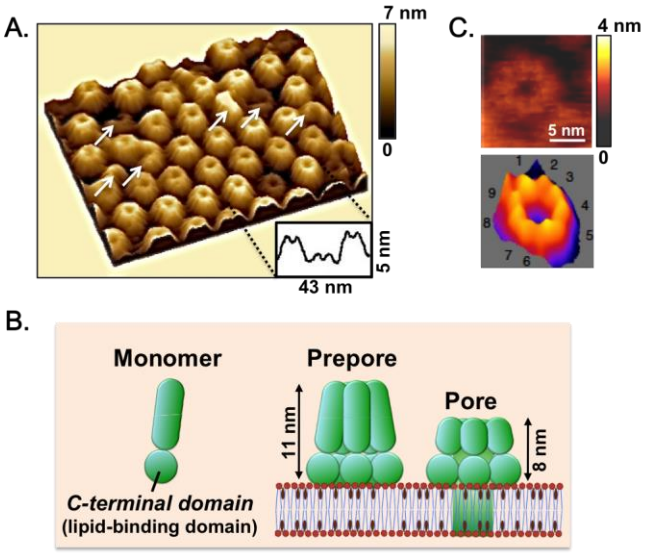

Fig. 1. Lysenin oligomers.

(A) Three-dimensional AFM height image of the hcp assembly of lysenin oligomers on SM/Chol (1/1) (mol/mol) bilayer with the height profile (inset) **[13]**. Arrows indicate the arc-shaped oligomers. **(B)** Illustration of the lysenin prepore and pore on lipid bilayer. **(C)** Two-dimensional (top) and three-dimensional (bottom) AFM height images of the lysenin oligomer **[21]**.

Figure 2. Yilmaz

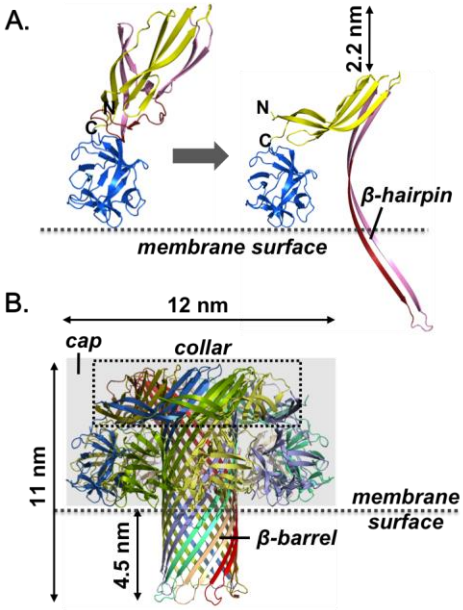

Fig. 2. Formation of lysenin pore **[21]**.

(A) The conformational change and the vertical collapse in lysenin protomer upon prepore-to- pore conversion. Yellow, pink-red and blue parts represent the N-terminal domain, the parts forming the β-hairpin and the C-terminal domain, respectively. The dotted grey lines indicate the position of the membrane surface. **(B)** Crystal structure of the lysenin pore. The dotted box and the bigger gray box encompass the collar and the cap, positioned above the membrane surface, respectively. Each protomer in the oligomer is represented by a different color.

Figure 3. Yilmaz

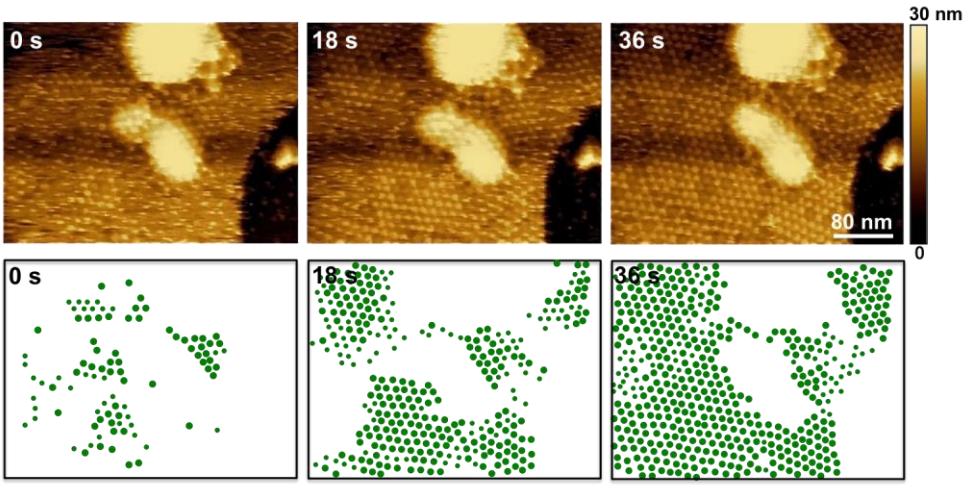

Fig. 3. Organization of lysenin oligomers.

Time-lapse AFM height images **(top)** and their schematic illustration **(bottom)** showing the formation of the hcp assembly of lysenin oligomers on SM/Chol (1/1) (mol/mol) bilayer **[13]**. Each lysenin oligomer is depicted in green in the illustration. The patches of very intense signal high above the membrane are the liposomes which did not fuse during the preparation of the supported lipid membrane.

Figure 4. Yilmaz

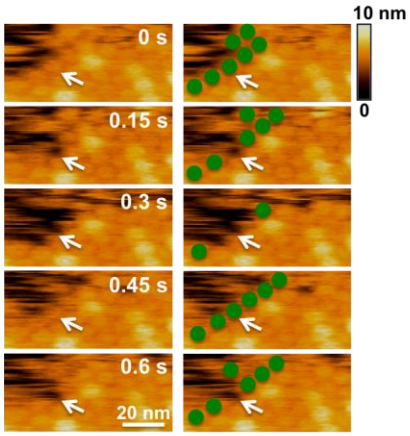

Fig. 4. Subsecond dynamics of lysenin oligomers.

Time-lapse AFM height images showing the dynamics of lysenin oligomers at the edge of the hcp assembly on SM/Chol (1/1) (mol/mol) bilayer **[13]**. The oligomers at the assembly edge are depicted in green in the images to the right. Arrows indicate an oligomer dissociating and reassociating.

Figure 5. Yilmaz

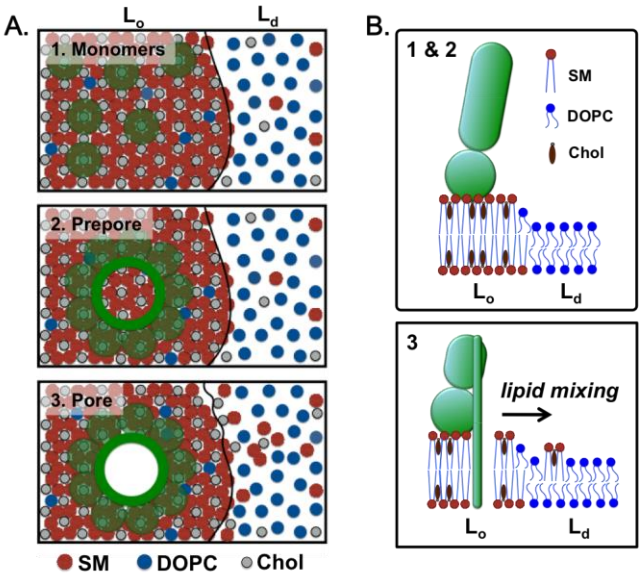

Fig. 5. Illustration of lysenin-induced membrane reorganization.

Top view **(A)**, adapted from **[16]**, and side view **(B)** of lipid distribution in the presence of lysenin monomers **(1)**, prepores **(2)** and pores **(3)**.